

Projections of temperature-attributable mortality in Europe: a time series analysis of 147 contiguous regions in 16 countries



Erica Martínez-Solanas*, Marcos Quijal-Zamorano*, Hicham Achebak, Desislava Petrova, Jean-Marie Robine, François R Herrmann, Xavier Rodó, Joan Ballester



Summary

Background Europe has emerged as a major climate change hotspot, both in terms of an increase in seasonal averages and climate extremes. Projections of temperature-attributable mortality, however, have not been comprehensively reported for an extensive part of the continent. Therefore, we aim to estimate the future effect of climate change on temperature-attributable mortality across Europe.

Methods We did a time series analysis study. We derived temperature-mortality associations by collecting daily temperature and all-cause mortality records of both urban and rural areas for the observational period between 1998 and 2012 from 147 regions in 16 European countries. We estimated the location-specific temperature-mortality relationships by using standard time series quasi-Poisson regression in conjunction with a distributed lag non-linear model. These associations were used to transform the daily temperature simulations from the climate models in the historical period (1971–2005) and scenario period (2006–2099) into projections of temperature-attributable mortality. We combined the resulting risk functions with daily time series of future temperatures simulated by four climate models (ie, GFDL-ESM2M, HadGEM2-ES, IPSL-CM5A-LR, and MIROC5) under three greenhouse gas emission scenarios (ie, Representative Concentration Pathway [RCP]2.6, RCP6.0, and RCP8.5), providing projections of future mortality attributable fraction due to moderate and extreme cold and heat temperatures.

Findings Overall, 7·17% (95% CI 5·81–8·50) of deaths registered in the observational period were attributed to non-optimal temperatures, cold being more harmful than heat by a factor of ten (6·51% [95% CI 5·14–7·80] vs 0·65% [0·40–0·89]), and with large regional differences across countries—eg, ranging from 4·85% (95% CI 3·75–6·00) in Germany to 9·87% (8·53–11·19) in Italy. The projection of temperature anomalies by RCP scenario depicts a progressive increase in temperatures, more exacerbated in the high-emission scenario RCP8.5 (4·54°C by 2070–2099) than in RCP6.0 (2·89°C) and RCP2.6 (1·67°C). This increase in temperatures was transformed into attributable fraction. Projections consistently indicated that the increase in heat attributable fraction will start to exceed the reduction of cold attributable fraction in the second half of the 21st century, especially in the Mediterranean and in the higher emission scenarios. The comparison between scenarios highlighted the important role of mitigation, given that the total attributable fraction will only remain stable in RCP2.6, whereas the total attributable fraction will rapidly start to increase in RCP6.0 by the end of the century and in RCP8.5 already by the middle of the century.

Interpretation The increase in heat attributable fraction will start to exceed the reduction of cold attributable fraction in the second half of the 21st century. This finding highlights the importance of implementing mitigation policies. These measures would be especially beneficial in the Mediterranean, where the high vulnerability to heat will lead to an imbalance between the decreasing cold and increasing heat-attributable mortality.

Funding None.

Copyright © 2021 The Author(s). Published by Elsevier Ltd. This is an Open Access article under the CC BY-NC-ND 4.0 license.

Introduction

The increase in the concentration of anthropogenic greenhouse gases in the atmosphere has led to a detectable planetary warming since the mid-20th century.¹ The general rise in temperatures and the associated increase in the intensity, frequency, and duration of heatwaves are expected to have a direct contribution on human mortality.^{2,3} Most studies project an increase in heat-attributable deaths and a concurrent decrease in

cold-attributable mortality under different scenarios of greenhouse gas emissions, resulting in a positive or negative long-term net effect depending on the location and magnitude of the warming.⁴ However, the variation in heat-attributable mortality is subject to large sources of uncertainty, especially regarding the capacity of societies to adapt to warmer conditions.^{5,6} Indeed, reductions in mortality risk and burden associated with heat have been documented over the past decades in many locations

Lancet Planet Health 2021;
5: e446–54

*Contributed equally

ISGlobal, Barcelona, Spain
(È Martínez-Solanas PhD,
M Quijal-Zamorano MSc,
H Achebak PhD, D Petrova PhD,
Prof X Rodó PhD, J Ballester PhD);
Centre for Demographic
Studies, Autonomous
University of Barcelona,
Barcelona, Catalonia, Spain
(H Achebak); Institut National
de la Santé et de la Recherche
Médicale (INSERM),
Montpellier, France
(Prof J-M Robine PhD); École
Pratique des Hautes Études,
Paris, France (Prof J-M Robine);
Division of Geriatrics,
Department of Rehabilitation
and Geriatrics, Geneva
University Hospitals and
University of Geneva, Thônex,
Switzerland
(Prof F R Herrmann MD); ICREA,
Barcelona, Spain (Prof X Rodó)

Correspondence to:
Mr Marcos Quijal-Zamorano,
ISGlobal, 08003 Barcelona, Spain
marcos.quijal@isglobal.org

Research in context**Evidence before this study**

Several studies have shown the effect of projected warming on future temperature-attributable mortality in Europe. Previous results indicate a general increase in attributable deaths due to heat and a decrease in attributable deaths due to cold, under different greenhouse gas emission scenarios. However, these studies are limited to the urban population from a subset of European countries, which limits the scope of the spatial description of the future projections in temperature-attributable mortality across the continent.

Added value of this study

One of the strengths of this study is the use of a unique, format-homogeneous, 15-year mortality dataset for 147 contiguous regions in 16 European countries, including deaths from both urban and rural areas. The broad geographical coverage of our European domain gives an

opportunity to estimate the effects and spatial distribution of rising temperatures in the continent.

Implications of all the available evidence

Our projections indicate a generalised reduction in cold-attributable mortality and an increase in heat-attributable mortality. However, although cold-attributable mortality was relatively homogeneous among regions, heat-attributable mortality was higher in the Mediterranean, and especially by the end of the 21st century and under Representative Concentration Pathway [RCP]8.5. The comparison between scenarios highlighted the important role of mitigation, given that temperature-attributable mortality will only remain stable in RCP2.6, whereas temperature-attributable mortality will rapidly start to increase in RCP6.0 by the end of the century and in RCP8.5 already by the middle of the century. Evidence from this study could inform scenario-based climate change mitigation strategies in Europe.

across the globe, mainly in developed countries, despite the already observed warming and the ageing of societies.^{7–10}

Europe has emerged as a major climate change hotspot, both in terms of an increase in seasonal averages and climate extremes.¹¹ The temperature increase in this region has occurred at a rate faster than in any other continent in recent decades, with 2020 being the warmest year on record at more than 1·6°C above the period between 1981 and 2010.¹² Record-breaking temperatures such as those recorded during summer 2003, which are representative of the future summer conditions in the region,⁵ had an unprecedented impact on mortality across the continent, causing more than 70 000 premature deaths in Europe alone.¹³ However, the distribution of the incidence was not spatially homogeneous. Although temperature anomalies were, for example, twice as large in France as in Spain, the largest relative excess of mortality occurred in Spain, showing the different degree of vulnerability of the European societies to anomalously warm summer temperatures.⁵ Therefore, in this study, we aim to estimate the future effect of climate change on temperature-attributable mortality across Europe.

Methods**Study design and definition of periods**

We did a time series analysis study. We used daily temperature and mortality records in the observational period (1998–2012) to derive temperature-mortality associations. These associations were used to transform the daily temperature simulations from the climate models in the historical period (1971–2005) and scenario period (2006–2099) into projections of temperature-attributable mortality. We calculated the changes in temperature and temperature-attributable mortality by comparing differences between the 30-year reference (1976–2005), mid-century (2035–2064), and

end-of-the-century (2070–2099) periods. All periods include data from all months—ie, from Jan 1 to Dec 31.

Mortality data

We used a daily mortality database that was spatio-temporally homogeneous, with nearly 60 million counts of deaths. The daily mortality counts consisted of all-cause mortality for the observational period (ie, between 1998 and 2012) from 147 contiguous regions (mainly NUTS2, ie, second level of the Nomenclature of Territorial Units for Statistics) in 16 European countries representing an urban and rural population of about 420 million people (appendix p 3).^{14,15} These countries are Austria (n=9 regions), Belgium (n=11), Croatia (n=2), Czech Republic (n=8), Denmark (n=1), France (n=22), Germany (n=16), Italy (n=21), Luxembourg (n=1), the Netherlands (n=1), Poland (n=16), Portugal (n=5), Slovenia (n=1), Spain (n=16), Switzerland (n=7) and the UK (n=10 regions in England and Wales only).

The method used to collect death counts was equivalent in all the countries; therefore, the dataset does not present data quality differences that could produce significant biases in time or across national or regional borders. The dataset had no missing values. Further details are provided in the appendix (p 2) and previously published studies.^{14,15}

Temperature data

Daily high-resolution gridded observations ($0\cdot25^\circ \times 0\cdot25^\circ$) of daily mean 2-meter temperature were derived from E-OBS (version 14.0).¹⁶ Time series of daily mean 2-meter temperature for the historical and scenario periods were derived from the second phase of the Inter-Sectoral Impact Model Intercomparison Project (ISIMIP2b),¹⁷ and bias-corrected with respect to the E-OBS data in the observational period by using an additive scaling method.^{18–21} We included data from four climate

For more on the Nomenclature of Territorial Units for Statistics see <https://ec.europa.eu/eurostat/web/nuts/background>

See Online for appendix

models—namely, GFDL-ESM2M, HadGEM2-ES, IPSL-CM5A-LR, and MIROC5—and three greenhouse gas emission scenarios (Representative Concentration Pathway [RCP]2.6, RCP6.0, and RCP8.5). Both sources of gridded temperature data were transformed into regional estimates by spatially averaging the gridded data within each region.

Estimation of temperature-mortality relationships

We first applied a standard time-series quasi-Poisson regression in combination with a distributed lag non-linear model^{10,22} in each region to derive estimates of region-specific temperature-mortality associations, reported as relative risks (RRs). The equation is as follows:

$$\text{Log}(E(Y)) = \text{intercept} + S(\text{time}, 8 \text{ df per year}) + \text{dow} + \text{cb}$$

Y denotes the daily time series of mortality counts; E corresponds to the expected value; S is a natural cubic spline of time with 8 degrees of freedom (df) per year to adjust for the seasonal and long-term trends; dow corresponds to a categorical variable to control for the

day of the week; and cb is the cross-basis function produced by the distributed lag non-linear model that combines the exposure-response and lag-response associations.⁴ The exposure-response association was modelled with a natural cubic spline, with three internal knots placed at the 10th, 75th, and 90th percentiles of the daily temperature distribution in the observational period. The lag-response association was modelled with three internal knots placed at equally spaced intervals in the log scale, with a maximum lag of 21 days to account for the long-delayed effects of cold temperatures and short-term harvesting. The modelling choices were tested in sensitivity analyses by varying the number of knots in the exposure-response function, the number of lag days, and the number of df per year used to control for the seasonal and long-term trends (appendix pp 7–9).

In the second stage, we did a multivariate multilevel meta-analysis, modelling dependencies of regions within countries through structured random effects.^{23,24} The fitted meta-analytical model was also used to derive the best linear unbiased predictions of the temperature-mortality relationships and the minimum

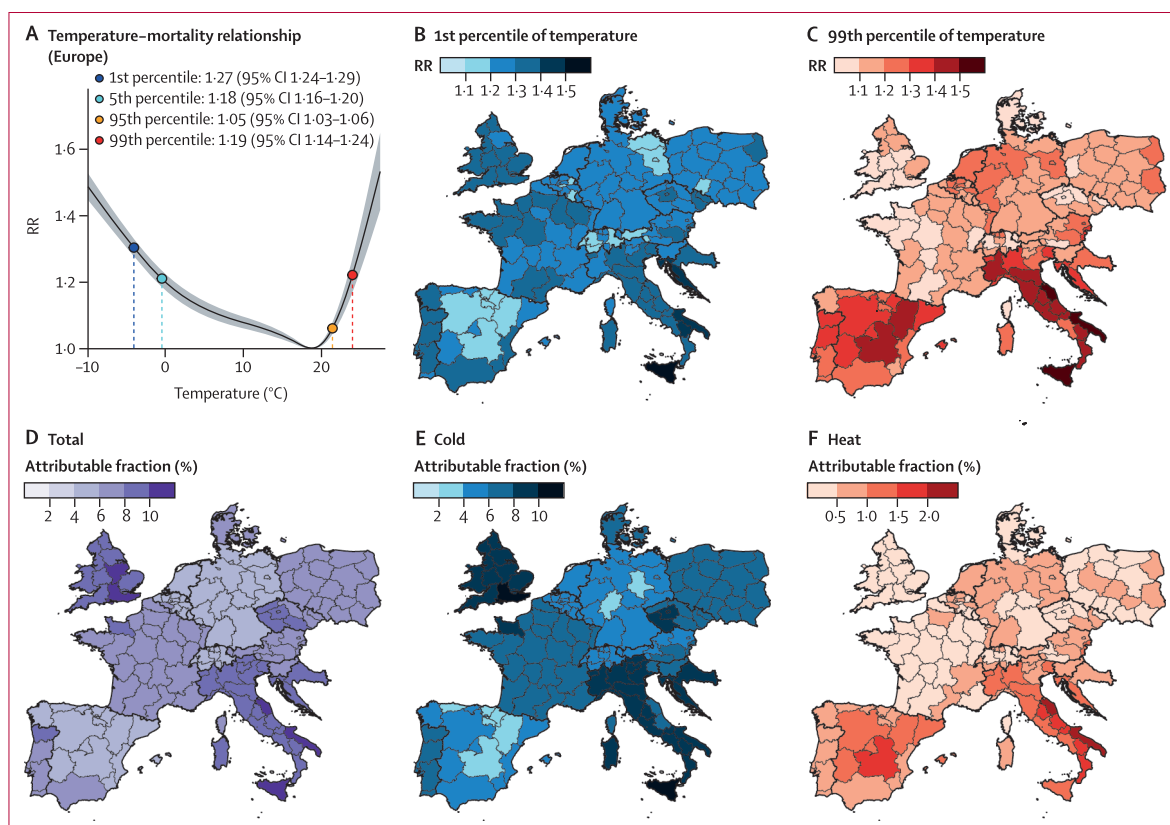


Figure 1: RR and attributable fraction in the observational period (1998–2012)

(A) Overall cumulative temperature-mortality relationship in Europe. The shaded area is the 95% CI. The RR was 1.27 (95% CI 1.24–1.29) in the 1st percentile, 1.18 (1.16–1.20) for the 5th percentile, 1.05 (1.03–1.06) for the 95th percentile, and 1.19 (1.14–1.24) for the 99th percentile. (B) RR of death at the 1st percentile of daily temperatures. (C) RR of death at the 99th percentile of daily temperatures. (D) Total attributable fraction. (E) Cold attributable fraction. (F) Heat attributable fraction. RR=relative risk.

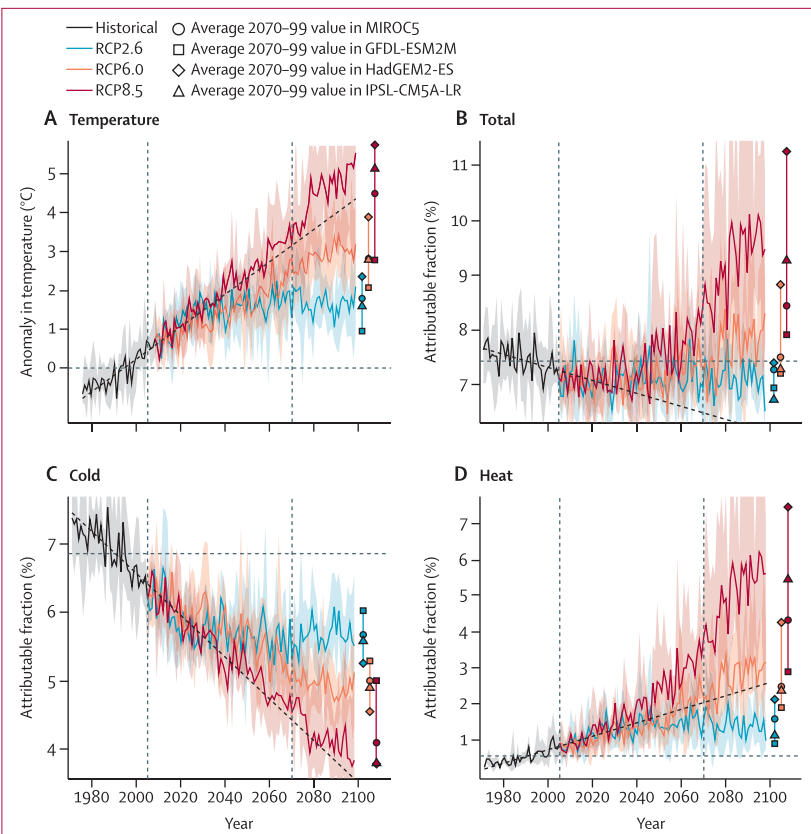


Figure 2: Projections of temperature anomaly and attributable fraction by RCP scenario in Europe
 (A) Annual mean temperature expressed as the anomaly with respect to the reference period (1976–2005).
 (B) Attributable fraction corresponding to all temperatures. (C) Attributable fraction corresponding to cold temperatures. (D) Attributable fraction corresponding to heat temperatures. Projections correspond to the average of the four models. The shaded areas are the CIs to the range of the ensemble of models. The dashed black lines correspond to the extrapolation of the linear trend in the reference period (1976–2005). RCP=Representative Concentration Pathway.

mortality temperature in each region. The fraction of deaths attributable to non-optimal temperatures (ie, attributable fraction) in each region was calculated following the methodology used in a previously published model.²⁵ Continental and national attributable fraction values were computed by integrating the regional values. 95% CIs of attributable risk were obtained empirically through 1000 Monte Carlo simulations.

Cold and heat days were defined as the days with temperatures lower or higher than the minimum mortality temperature. These subsets of days were further divided into extreme cold (cold days colder than 2·5 percentile in the observational period), moderate cold (cold days warmer than 2·5 percentile), moderate heat (heat days colder than 97·5 percentile), and extreme heat (heat days warmer than 97·5 percentile). The thresholds used to define moderate and extreme cold and heat days were calculated during the observational period, and applied to all the periods (observational, historical, and scenario).

Projections of temperature-attributable mortality

Similar to previous studies,^{4,26} we used the mean annual cycle of daily mortality in the observational period as the baseline mortality in the historical and scenario periods. We thus computed the projected attributable fraction in each region by combining the fitted exposure-response curves derived from the observational period with the multi-model ensemble of bias-corrected daily temperature time series.²⁷ Projected attributable fraction values were calculated as the average of the multi-model ensemble. Projected attributable fractions CIs were calculated as the range of the multi-model ensemble. The attributable fraction projections were obtained under the assumption of no adaptation or population changes.

We did all statistical analyses using R (version 4.0.4) with the packages dlnm (version 2.4.2) and mixmeta (version 1.1.0).

Role of the funding source

There was no funding source for this study. All authors had full access to all the data in the study and had final responsibility for the decision to submit for publication.

Results

Figure 1A shows the pooled cumulative exposure-response association for the whole ensemble of regions over the observational period. The association corresponds to an asymmetric V-shaped curve, with monotonically increasing risks for temperatures colder and warmer than the optimum temperature. For example, the risk of death increases by 27% at the 1st percentile, 18% at the 5th percentile, 5% at the 95th percentile, and 19% at the 99th percentile of the daily temperature distribution, with a much steeper slope for heat than for cold. Figure 1B and C depict the regional RRs corresponding to the 1st and 99th percentiles of the daily temperature distribution. The whole ensemble of regional RR curves is shown in the appendix (pp 10–15). For cold temperatures, the RRs are high and relatively homogeneous in most of the domain, except in some regions in the Mediterranean and central Europe (figure 1B). Instead, large latitudinal differences are found for warm temperatures, with the largest RRs in the Mediterranean (figure 1C). Interestingly, we observed large discontinuities for both cold and heat across national borders. For example, for heat, we find an abrupt transition between France and the neighbouring regions in Spain and Italy. Overall, 7·17% (95% CI 5·81–8·50; figure 1D) of the observed deaths are attributable to non-optimal temperatures, approximately ten times higher for cold than for heat (6·51% [95% CI 5·14–7·80] vs 0·65% [0·40–0·89]; figure 1E and F; appendix p 4). The attributable fraction due to all temperatures is largely heterogeneous across countries, ranging from 4·85% (95% CI 3·75–6·00) in Germany to 9·87% (8·53–11·19) in Italy. In general, the spatial patterns of attributable fraction resemble those of the RRs, with high and

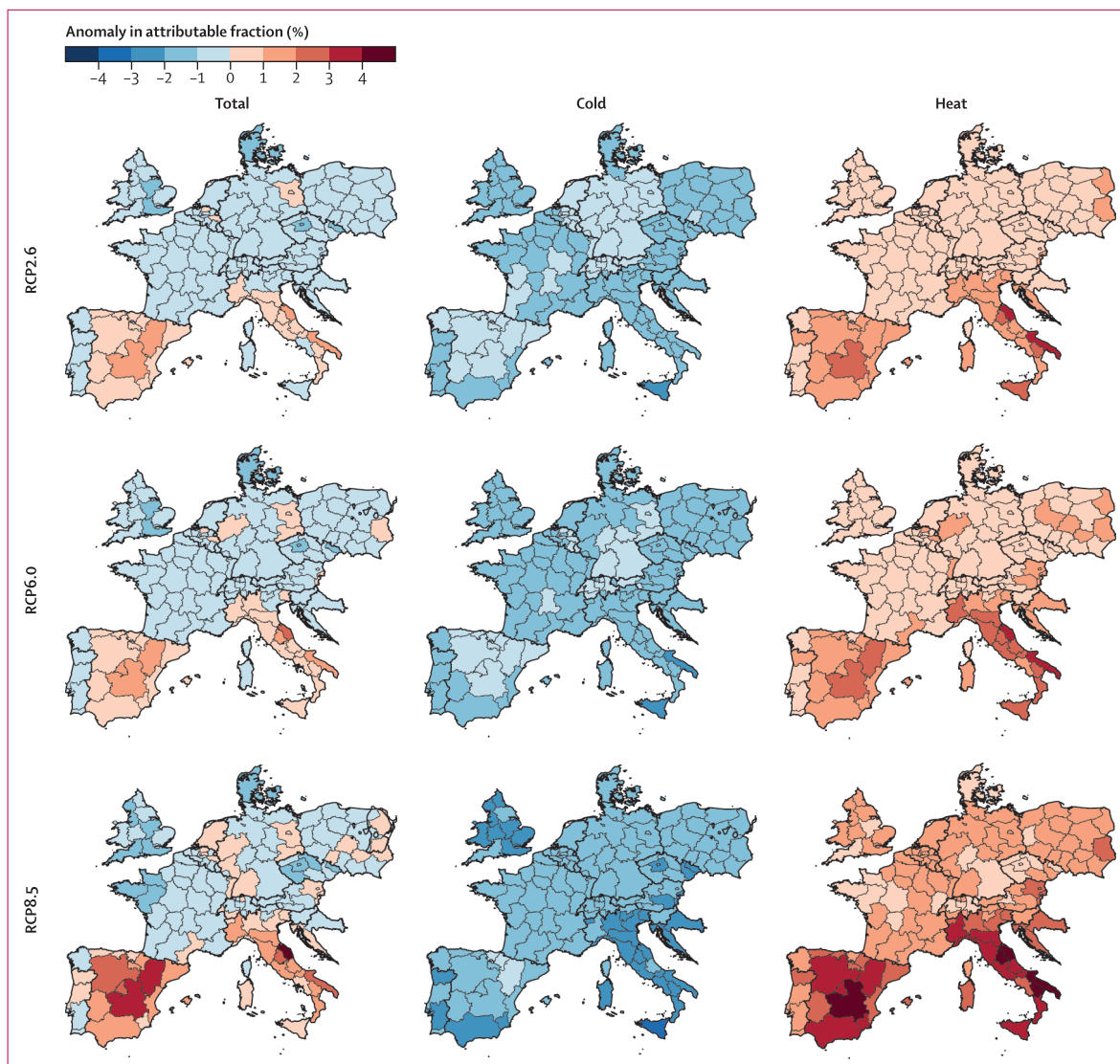


Figure 3: Attributable fraction anomalies by RCP scenario in the middle of the 21st century (2035–2064)

Anomalies are calculated as the average of the four models, and expressed with respect to the reference period (1976–2005). RCP=Representative Concentration Pathway.

relatively homogeneous cold-attributable mortality in most of the domain, but higher heat-attributable mortality in the Mediterranean compared with higher latitudes (figure 1).

Figure 2A depicts the projection of temperature anomalies by RCP scenario. It shows a progressive increase in temperatures, more exacerbated in the high-emission scenario RCP8.5 (4.54°C by 2070–2099) than in RCP6.0 (2.89°C) and RCP2.6 (1.67°C ; appendix pp 5–6). This increase in temperatures is transformed into attributable fraction values by means of the regional non-linear cumulative-response associations shown in the appendix (pp 10–15). As a result of the warming, we observed a decrease in the number of cold days and a complementary increase in the number of heat days, which leads to a progressive decrease in cold

attributable fraction and a progressive increase in heat attributable fraction. More specifically for cold, we found that the rather linear decline in RCP8.5 approximately mimics the linear trend defined by the reference period, whereas RCP2.6 and RCP6.0 approximately start to diverge from the linear trend at around year 2040 (figure 2C). For heat, RCP6.0 is instead the scenario that follows the linear trend defined by the reference period, with a faster increase in RCP8.5 and a slower growth in RCP2.6 (figure 2D). The resulting evolution of the total attributable fraction, which results from the combination of the cold and heat components, indicates a plateau in RCP2.6 throughout the present century, but a rapid increase starting in 2060 in RCP6.0 and in 2040 in RCP8.5 (figure 2B). Importantly, the total attributable fraction

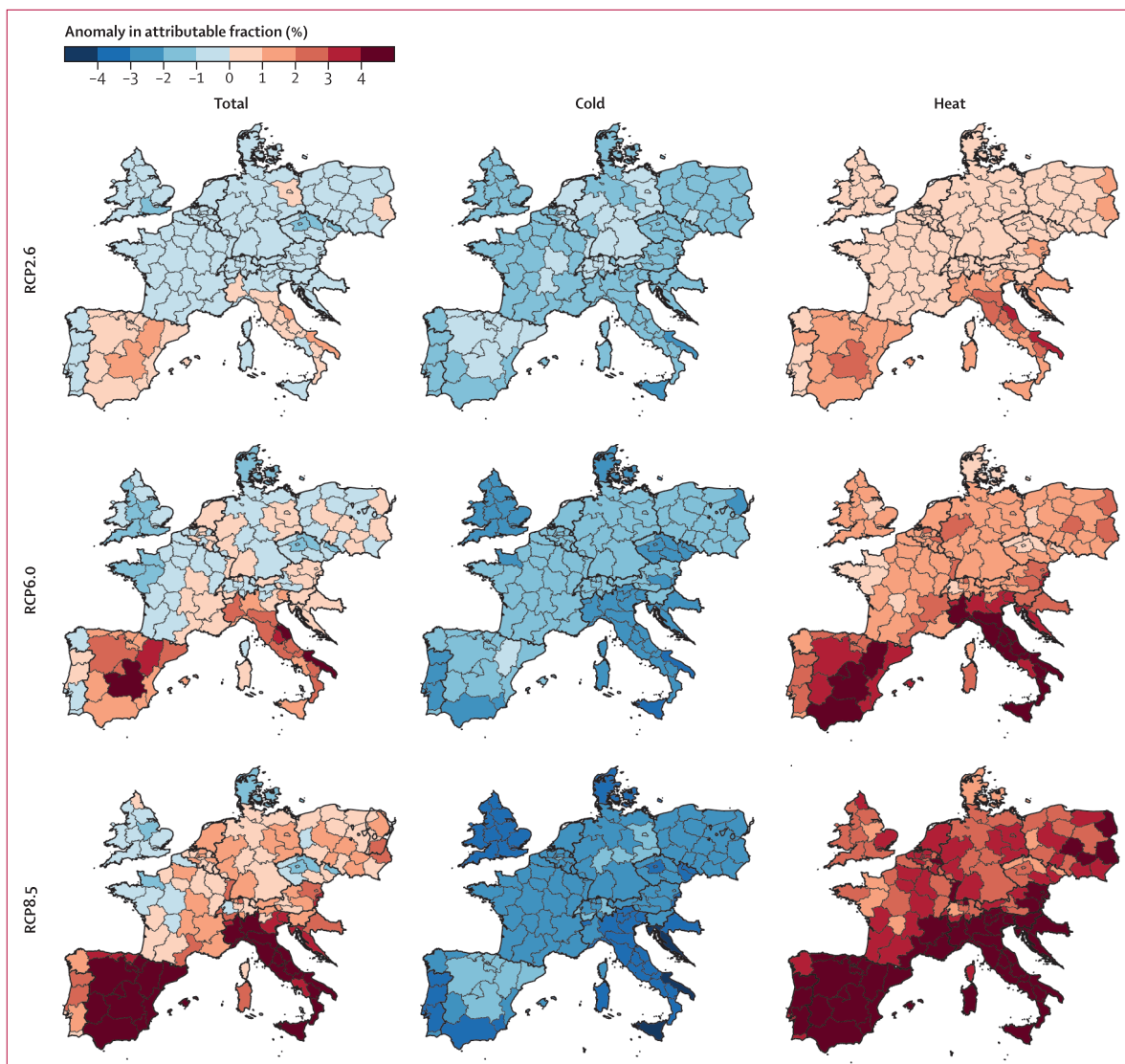


Figure 4: Attributable fraction anomalies by RCP scenario at the end of the 21st century (2070–2099)

Anomalies are calculated as the average of the four models, and expressed with respect to the reference period (1976–2005). RCP=Representative Concentration Pathway.

in all three scenarios exceed the evolution defined by the linear trend in the historical period.

Figures 3 and 4 show the projection anomalies of total, cold, and heat attributable fraction by RCP scenario at the middle and end of the 21st century. These spatial patterns resemble again the maps of cold and heat RR and attributable fractions in the observational period (figure 1). This resemblance is explained by the fact that projections of attributable fraction are largely driven by the observed regional differences in vulnerability among regions. To a lower extent, the attributable fraction anomalies are also explained by the different rate of warming among regions (appendix pp 40–41). For example, the large summer warming in the Mediterranean explains why the heat attributable fraction is expected to disproportionately increase in the

southern regions. Taking all these factors into account, the total attributable fraction largely increases in the south, and changes are relatively small in central Europe. The spatial pattern of attributable fraction anomalies is qualitatively similar in the mid-century and late-century periods, but the magnitude of the changes is substantially different.

Projections of cold and heat attributable fraction were further subcategorised into moderate and extreme temperatures (figure 5). The corresponding regional projections are provided in the appendix (pp 42–59). In the reference period, moderate cold accounts for most of the cold attributable fraction, whereas moderate and extreme heat attributable fraction are almost identical. In all the considered RCP scenarios, extreme cold attributable fraction is expected to decrease whereas

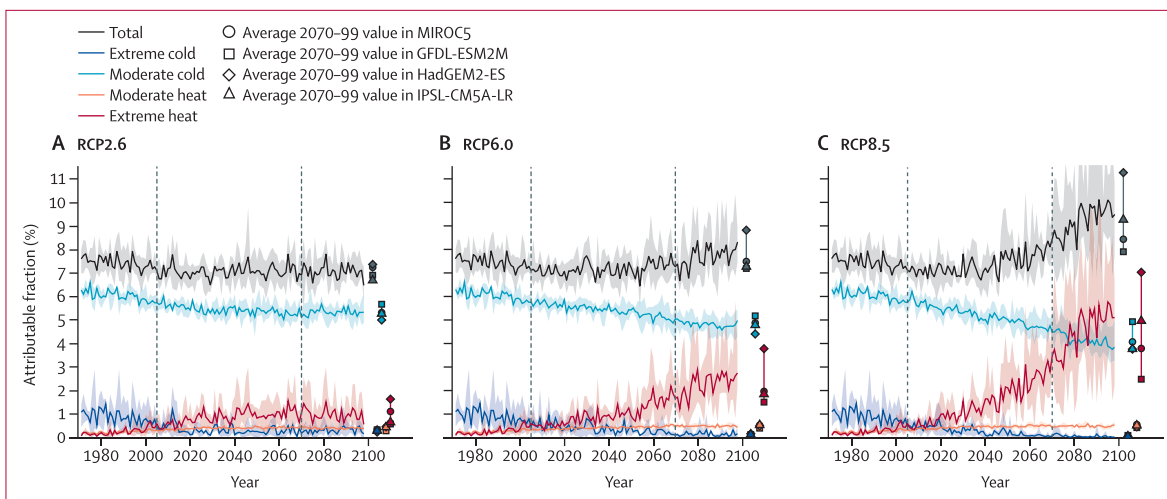


Figure 5: Projections of attributable fraction by RCP scenario in Europe

The attributable fraction is shown for all, extreme cold, moderate cold, moderate heat, and extreme heat temperatures. Projections correspond to the average of the four models. The shaded areas are CIs to the range of the ensemble of models. RCP=Representative Concentration Pathway.

moderate heat attributable fraction is expected to remain relatively constant. However, projections indicate a very large increase in extreme heat attributable fraction, which would surpass the cold attributable fraction in RCP8.5 by the end of the century (figure 5C).

Sensitivity analyses suggested that the results are consistent and did not depend on modelling choices (appendix pp 7–9).

Discussion

Our results show that 7·17% of the observed deaths in Europe are attributed to non-optimal temperatures, cold being more harmful than heat by a factor of ten, and with large regional differences across countries. Our projections indicate a generalised reduction in cold attributable fraction and an increase in heat attributable fraction. However, although cold attributable fraction was relatively homogeneous among regions, heat attributable fraction was clearly larger in the Mediterranean, and especially by the end of the century and under RCP8.5. The comparison between scenarios highlighted the important role of mitigation, given that the total attributable fraction will only remain stable in RCP2.6, whereas it will rapidly start to increase in RCP6.0 by the end of the 21st century, and in RCP8.5 already by the middle of the 21st century.⁵ One of the strengths of our study is the use of a unique, format-homogeneous, 15-year mortality dataset for 147 contiguous regions in 16 European countries, including deaths from both urban and rural areas. The broad geographical coverage of our European domain gives an opportunity to estimate the effects and spatial distribution of rising temperatures in the continent.

Although we estimated an overall negative net effect in total attributable fraction by the middle of the century, this effect was not the case for the end of the century,

when the rise in heat attributable fraction is expected to exceed the reduction in cold attributable fraction, especially for those scenarios considering little or no mitigation (RCP6.0 and RCP8.5). Our results are comparable with those reported elsewhere.^{4,5,26,28} The largest and most comparable study included data from six European countries with similar results to ours, in the sense that the rise in heat attributable fraction would exceed the reduction of cold attributable fraction in RCP8.5.⁴ Other authors have compared projections of temperature-attributable mortality under different magnitudes of global warming in a multi-country assessment²⁶ and in Germany.²⁸ They found similar estimations of changes in cold and heat attributable fraction, as well as a consistent increase in the net attributable fraction effect in most European countries.

The attributable fraction projections are mainly determined by the magnitude and timing of the warming and the transformation of temperatures into attributable fraction values by means of the exposure-response associations. These associations are in turn characterised by the position of the minimum mortality temperature and the slopes of the curve in the cold and heat tails. In the historical period, the decreasing trend in cold attributable fraction is found to be larger than the increasing trend in heat attributable fraction, resulting in a decreasing trend in the total attributable fraction. Assuming no adaptation, this decreasing trend in total attributable fraction is mainly due to the warming shift of the temperature distribution towards the minimum mortality temperature, which by definition corresponds to the point of the minimum RR, thus slowly reducing the total attributable fraction. At higher warming levels, however, other factors start to have an important role in the opposite direction, such as the higher slope of the exposure-response associations in the warm tail

compared with the one in the cold tail. Thus, the total attributable fraction starts to increase in RCP6.0 at the end of the century, or in RCP8.5 at the middle of the century. This effect is explained by the fact that the increase in heat attributable fraction due to the new heat days exceeds the decrease in cold attributable fraction due to the combination of two factors: the reduction in the number of cold days and the increase in the frequency of days with temperatures near the minimum mortality temperature. This point of inflection due to the non-linear transformation of temperatures into attributable fraction values by means of the exposure-response associations explains why the temperatures in the RCP6.0 and RCP8.5 scenarios approximately follow the linear trend defined by the historical period, whereas the corresponding total attributable fraction projections quickly diverge from the linear trend and suddenly start to increase during the second half of the century after a transition plateau. We refer to Ballester and colleagues⁵ for a more in-depth discussion of these processes.

We decided to report the temperature and attributable fraction anomalies as averages for 30-year periods, contrary to previous epidemiological studies that used shorter periods of 10 years.⁴⁷ The natural decadal climate variability can partially mask or amplify the real magnitude of the anthropogenic warming trends. Our year-to-year projections of temperature and attributable fraction actually show this natural decadal variability, even when looking at the averages of the four models (eg, see the anomalously warm temperature in RCP8.5 around 2076–2085). Thus, the use of 30-year periods in our study avoids this kind of misleading effect, and better allows to estimate the long-term trend of temperature and attributable fraction. For this reason, climate scientists use 30-year periods for the reference and scenario periods, as recommended by the World Meteorological Organization.²⁹

This study has some limitations worth acknowledging. First, our projections did not account for adaptation or demographic changes, in line with similar previously published studies.^{4,26,28} Projections based on idealised scenarios of adaptation can only be occasionally found in the literature.⁵ However, there is a growing amount of evidence pointing to adaptation processes already reducing the vulnerability to cold and heat.^{9,27} If we assumed in the projections the same rate of adaptation as in these studies, we would expect a smaller decrease in cold attributable fraction and a smaller increase in heat attributable fraction compared with the results presented here. Second, we showed the epidemiological confidence intervals for the observational period, but we prioritised reporting the spread of the multi-model ensemble in the projections to show the same type of information for temperature and attributable fraction. In general, we found smaller uncertainties in the epidemiological associations compared with the temperature spread of the multi-model ensemble. We note that this range would be much larger if

we used the very large ensemble of climate models from the Coupled Model Intercomparison Project initiative used in the Intergovernmental Panel on Climate Change reports. Third, daily mean temperature was used as the only environmental exposure, and we did not consider other parameters such as relative or absolute humidity. Some studies have found little differences in the amount of variability explained by the epidemiological models when humidity is included.³⁰ At climate change timescales, however, the European regions that will warm the most are also the regions that will dry faster (eg, the Mediterranean).⁵ By contrast, from a physiological perspective, heat stress is often thought of as a combination of high temperature and high humidity. Therefore, an epidemiological model driven by temperature alone, and thus ignoring an eventual decrease in humidity, might overestimate the future heat attributable fraction, especially in regions such as the Mediterranean. A more in-depth discussion of these factors is provided elsewhere,⁵ where the contribution of humidity to the projections of attributable mortality is quantified.

In conclusion, our results show that the increase in heat attributable fraction will start to exceed the reduction of cold attributable fraction in the second half of the 21st century, especially in the Mediterranean and in the higher emission scenarios. These findings highlight the importance of implementing mitigation policies across Europe. These measures would be especially beneficial in the Mediterranean, where the increase in the heat-attributable mortality is expected to be largely sensitive to the pathway of greenhouse gas emissions.

Contributors

ÈM-S, MQ-Z, and JB designed the study. ÈM-S, DP, FRH, J-MR, XR, and JB collected the data. ÈM-S, MQ-Z, HA, DP, and JB analysed and interpreted the data. FRH and JB verified the mortality and population data. ÈM-S, MQ-Z, DP, and JB verified the temperature data. ÈM-S, MQ-Z, HA, and JB wrote the manuscript. All authors had full access to all the data in the study, had the final responsibility for the decision to submit for publication, and approved the final version of this Article to be published.

Declaration of interests

We declare no competing interests.

Data sharing

No additional data are available for this Article.

Acknowledgments

MQ-Z, HA, DP, and JB gratefully acknowledge funding from the EU's Horizon 2020 research and innovation programme under grant agreement no 865564 (European Research Council Consolidator Grant EARLY-ADAPT). MQ-Z, ÈM-S, DP, and JB gratefully acknowledge funding from the EU's Horizon 2020 research and innovation programme under grant agreement no 727852 (project Blue-Action). HA gratefully acknowledges funding from the Secretariat for Universities and Research of the Ministry of Business and Knowledge of the Government of Catalonia (grant numbers B00391 [FI-2018], B100180 [FI-2019], and B200139 [FI-2020]). JB gratefully acknowledges funding from the EU's Horizon 2020 research and innovation programme under grant agreement no 956396 (project EDIPI), and from the Ministry of Science and Innovation (MCIU) under grant agreements no RYC2018-025446-I (programme Ramón y Cajal) and EUR2019-103822 (project EURO-ADAPT). JR gratefully acknowledges funding from the EU Community Action Program for Public Health (grant agreement no 2005114). ISGlobal acknowledges support from the Spanish Ministry of

Science and Innovation through the Centro de Excelencia Severo Ochoa 2019–2023 Program (CEX2018-000806-S) and support from the Generalitat de Catalunya through the CERCA programme. The authors also acknowledge the E-OBS dataset from the EU-FP6 project UERRA and the Copernicus Climate Change Service, and the data providers in the ECA&D project. For their roles in producing, coordinating, and making available the Inter-Sectoral Impact Model Intercomparison Project (ISIMIP) input data and impact model output, the authors acknowledge the modelling groups, the ISIMIP sector coordinators, and the ISIMIP cross-sectoral science team for the health sector.

References

- 1 The Intergovernmental Panel on Climate Change. Special report: global warming of 1·5°C. 2018. <https://www.ipcc.ch/sr15/> (accessed May 25, 2021).
- 2 Perkins-Kirkpatrick SE, Lewis SC. Increasing trends in regional heatwaves. *Nat Commun* 2020; **11**: 3357.
- 3 Watts N, Amann M, Ayeb-Karlsson S, et al. The *Lancet* Countdown on health and climate change: from 25 years of inaction to a global transformation for public health. *Lancet* 2018; **391**: 581–630.
- 4 Gasparini A, Guo Y, Sera F, et al. Projections of temperature-related excess mortality under climate change scenarios. *Lancet Planet Health* 2017; **1**: e360–67.
- 5 Ballester J, Robine J-M, Herrmann FR, Rodó X. Long-term projections and acclimatization scenarios of temperature-related mortality in Europe. *Nat Commun* 2011; **2**: 358.
- 6 Huang C, Barnett AG, Wang X, Vaneckova P, FitzGerald G, Tong S. Projecting future heat-related mortality under climate change scenarios: a systematic review. *Environ Health Perspect* 2011; **119**: 1681–90.
- 7 Vicedo-Cabrera AM, Sera F, Guo Y, et al. A multi-country analysis on potential adaptive mechanisms to cold and heat in a changing climate. *Environ Int* 2018; **111**: 239–46.
- 8 Achebak H, Devolder D, Ballester J. Heat-related mortality trends under recent climate warming in Spain: a 36-year observational study. *PLoS Med* 2018; **15**: e1002617.
- 9 Achebak H, Devolder D, Ballester J. Trends in temperature-related age-specific and sex-specific mortality from cardiovascular diseases in Spain: a national time-series analysis. *Lancet Planet Health* 2019; **3**: e297–306.
- 10 Achebak H, Devolder D, Vijendra V, Ballester J. Reversal of the seasonality of temperature-attributable mortality from respiratory diseases. *Nat Commun* 2020; **11**: 2457.
- 11 Giorgi F. Climate change hot-spots. *Geophys Res Lett* 2006; **33**: L08707.
- 12 European State of the Climate. Climate indicators: temperature. 2020. <https://climate.copernicus.eu/climate-indicators/temperature> (accessed May 25, 2021).
- 13 Robine J-M, Cheung SLK, Le Roy S, et al. Death toll exceeded 70 000 in Europe during the summer of 2003. *C R Biol* 2008; **331**: 171–78.
- 14 Ballester J, Robine J-M, Herrmann FR, Rodó X. Effect of the Great Recession on regional mortality trends in Europe. *Nat Commun* 2019; **10**: 679.
- 15 Ballester J, Rodó X, Robine J-M, Herrmann FR. European seasonal mortality and influenza incidence due to winter temperature variability. *Nature Clim Change* 2016; **6**: 927–30.
- 16 Cornes RC, van der Schrier G, van den Besselaar EJM, Jones PD. An ensemble version of the E-OBS temperature and precipitation data sets. *J Geophys Res Atmos* 2018; **123**: 9391–409.
- 17 Warszawski L, Frieler K, Huber V, Piontek F, Serdeczny O, Schewe J. The Inter-Sectoral Impact Model Intercomparison Project (ISI-MIP): project framework. *Proc Natl Acad Sci USA* 2014; **111**: 3228–32.
- 18 Hempel S, Frieler K, Warszawski L, Schewe J, Piontek F. A trend-preserving bias correction—the ISI-MIP approach. *Earth Syst Dynam* 2013; **4**: 219–36.
- 19 Yuanchao X. hyfo: hydrology and climate forecasting. 2020. <https://CRAN.R-project.org/package=hyfo> (accessed May 25, 2021).
- 20 Santander Meteorology Group. downscaleR: an R package for bias correction and statistical downscaling. 2015. <https://github.com/SantanderMetGroup/downscaleR/wiki> (accessed May 21, 2021).
- 21 Wilcke RAI, Mendlik T, Gobiet A. Multi-variable error correction of regional climate models. *Climatic Change* 2013; **120**: 871–87.
- 22 Gasparini A, Armstrong B, Kenward MG. Distributed lag non-linear models. *Stat Med* 2010; **29**: 2224–34.
- 23 Sera F, Armstrong B, Blangiardo M, Gasparini A. An extended mixed-effects framework for meta-analysis. *Stat Med* 2019; **38**: 5429–44.
- 24 Vicedo-Cabrera AM, Sera F, Liu C, et al. Short term association between ozone and mortality: global two stage time series study in 406 locations in 20 countries. *BMJ* 2020; **368**: m108.
- 25 Gasparini A, Leone M. Attributable risk from distributed lag models. *BMC Med Res Methodol* 2014; **14**: 55.
- 26 Vicedo-Cabrera AM, Guo Y, Sera F, et al. Temperature-related mortality impacts under and beyond Paris Agreement climate change scenarios. *Clim Change* 2018; **150**: 391–402.
- 27 Vicedo-Cabrera AM, Sera F, Gasparini A. Hands-on tutorial on a modeling framework for projections of climate change impacts on health. *Epidemiology* 2019; **30**: 321–29.
- 28 Veronika H, Krummenauer L, Peña-Ortiz C, et al. Temperature-related excess mortality in German cities at 2°C and higher degrees of global warming. *Environ Res* 2020; **186**: 109447.
- 29 World Meteorological Organization. WMO guidelines on the calculation of climate normals. 2017. https://library.wmo.int/docnum.php?explnum_id=4166 (accessed May 25, 2021).
- 30 Armstrong B, Sera F, Vicedo-Cabrera AM, et al. The role of humidity in associations of high temperature with mortality: a multicountry, multicity study. *Environ Health Perspect* 2019; **127**: 97007.

For more on UERRA see
<http://www.uerra.eu>

For more on the ECA&D project see <https://www.ecad.eu>